

Report

Level Assignment for Various Photoluminescence Bands of Tm^{3+} Ions in LiYF_4 Crystal

Taiju TSUBOI^a
Hideyuki MURAYAMA^b
Masayuki TANIGAWA^c
Kiyoshi SHIMAMURA^d

^aResearch Institute of Advanced Technology, Kyoto Sangyo University,
Kamigamo, Kita-ku, Kyoto 603-8555, Japan

^bFaculty of Engineering, Kyoto Sangyo University

^cFaculty of Science, Kyoto Sangyo University

^dKagami Memorial Laboratory for Materials Science and Technology, Waseda University,
2-8-26 Nishiwaseda, Shinjuku-ku, Tokyo 169-0051, Japan

Abstract

Photoluminescence and excitation spectra of Tm^{3+} ions in LiYF_4 crystal have been investigated at 12 K. The luminescence is investigated under excitation with lights of 780, 680, 460, 360 and 266 nm wavelengths. The emission bands are observed to depend on the excitation wavelength, e.g. two emission bands at 1229 and 1201 nm are generated by the 460 nm excitation but not by 780, 680, 360 and 266 nm excitation. Comparing the emission spectra with the excitation spectra for the IR and visible emissions, we suggest the level assignment for the observed luminescence bands including the 288 and 286 nm UV emission bands.

1. Introduction

Tm^{3+} -doped crystals have been of interest because the infrared lasers of about 1.8 μm wavelength are important for medical applications¹⁻⁴. Tm^{3+} -doped crystals show an additional infrared emission at about 1.47 μm . Optical communication has been currently performed using lasers operating in 1.5 μm C-band region where silica fibers have low loss. The wavelength region of 1.45–1.50 μm is also a low-loss region. This wavelength region will be important in near future as it will enable us to extend the optical communication bandwidth to S-band region^{5,6}. Therefore Tm^{3+} -doped materials are useful as optical amplification device in the future optical communications.

Additionally the Tm^{3+} -doped crystals are of interest because they generate photoluminescence (PL) in ultraviolet, blue, green and red regions. Of various Tm^{3+} -doped crystals, Tm^{3+} -doped LiYF_4 (YLF) crystals are well known for the high efficient up-converted blue and red emissions^{7,9}. So far considerable amount of investigation has been made on the

PL of various Tm^{3+} -doped materials including single crystals and glasses. However few studies have been undertaken on the dependence of PL spectra on the excitation wavelength. For example, it is not clear whether 650–670 nm emission spectrum is generated equally by the excitations into the $^1\text{G}_4$, $^1\text{D}_2$ and $^3\text{P}_2$ states of Tm^{3+} .

Figure 1 shows the 1400–1525 nm IR emission spectra generated by the excitations with 780, 680, 460, 360 and 260 nm lights. The weak bands are observed at 1476, 1486 and 1488 nm in the spectrum observed by the 360 nm excitation, and the 1476 nm band is also observed by the 260 nm excitation. These 1476, 1486 and 1488 nm bands were attributed to the second harmonic emission bands. When we neglect the second harmonic bands, we find that the IR emission spectra do not depend on the excitation wavelength.

Figure 2 shows another example of the emission spectra at 770–840 nm region generated by the 780, 680, 460, 360 and 260 nm excitations. These excitations give rise to the 817, 809 and 797 nm emission bands, while the 460 nm excitation gives rise to two additional emission bands at 791 and 804 nm. The 817, 809 and 797 nm emission bands have been attributed to the $^3\text{H}_4 \rightarrow ^3\text{H}_6$ transition. It is interesting to determine the origin of the additional 791 and 804 nm emission bands. Unlike the case of 1400–1525 nm emission spectra, the 770–840 nm spectra depend on the excitation wavelength. Therefore it is interesting to investigate whether the excitation wavelength dependence is observed in the other IR and visible emission spectra. In the present paper we report the dependence of PL on the excitation wavelength. The investigation is undertaken for the PL at low temperature such as 12 K because one can obtain more detailed and clear spectra by the low temperature measurement than by the room temperature one.

Tm^{3+} ion has the $^3\text{F}_4$, $^3\text{H}_5$, $^3\text{H}_4$, $^3\text{F}_3$, $^3\text{F}_2$, $^1\text{G}_4$, $^1\text{D}_2$, $^1\text{I}_6$, $^3\text{P}_0$, $^3\text{P}_1$ and $^3\text{P}_2$ excited states⁹⁻¹². Of them the possible emitting states are the $^3\text{F}_4$, $^3\text{H}_4$, $^1\text{G}_4$, $^1\text{D}_2$ and $^1\text{I}_6$ because each of these

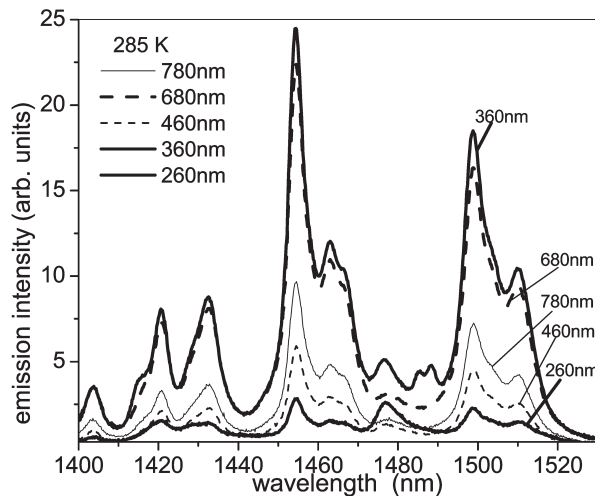


Fig. 1 IR emission spectra of 6% Tm^{3+} -doped LiYF_4 crystal excited by 780, 680, 460, 360 and 260 nm lights at 285 K.

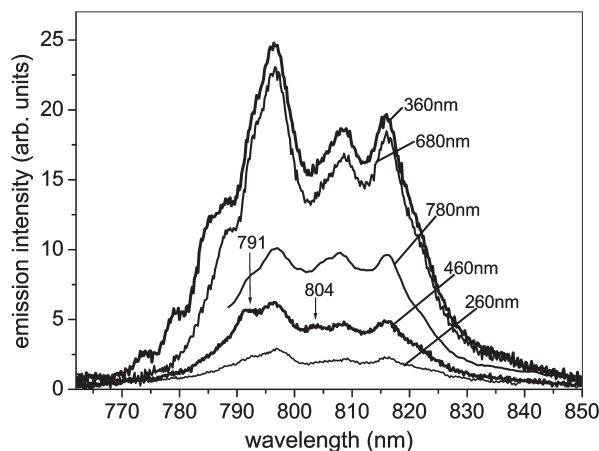


Fig. 2 Emission spectra of 6% Tm^{3+} -doped LiYF_4 crystal excited by 780, 680, 460, 360 and 260 nm lights at 285 K.

states (e.g. $^3\text{H}_4$) has a relatively large energy gap from its nearby low-energy state ($^3\text{H}_5$). Fluoride crystals have lower phonon energy than oxide crystals. The highest phonon energy is 556 cm^{-1} in YLF^{13} . Therefore all the emitting states are expected to give rise to emission because e.g. the gap between the $^1\text{I}_6$ state and its nearby low-energy $^1\text{D}_2$ states is so wide (about 7000 cm^{-1}) that the non-radiative multi-phonon relaxation is impossible in the transition from the $^1\text{I}_6$ state to the $^1\text{D}_2$ state. Additionally fluorides are more transparent (up to UV region) than oxides. Thus one can expect to observe the UV emission due to the transitions from the $^1\text{D}_2$ and $^1\text{I}_6$ states. The detailed study, however, has not been undertaken on those UV transitions even in YLF . In the present paper we study the high-energy luminescence, together with the dependence of PL on the excitation wavelength.

2. Experimental procedure

Single crystal of 6% Tm^{3+} -doped LiYF_4 (called TmYLF , hereafter) was grown in an RF-heating Czochralski furnace. High purity commercial yttrium fluoride, lithium fluoride and thulium fluoride were used as a starting materials in the crystal growth. These compounds were melted in an iridium crucible in the Czochralski furnace under atmosphere of CF_4 . Crystal was grown at a pulling rate of 1 mm/h and rotation rate of 15 rpm. After growth the crystal was cooled down to room temperature at a rate of $30^\circ\text{C}/\text{h}$. The Tm^{3+} concentration is $8.4 \times 10^{20}\text{ cm}^{-3}$. It was found that this crystal unintentionally contains a very small amount of Ho^{3+} ions (less than 0.01%).

The emission and excitation spectra were measured with a Spex Fluorolog-3 fluorophotometer in 350–1600 nm spectral region. The excitation was undertaken by 450 W Xe-lamp. The excitation wavelength was selected to be 780, 680, 460, 360 and 260 nm. A Lambda Vision Inc. ISM-140G instant spectrograph unit with an electrically cooled

InGaAs image sensor was used to measure the infrared emission spectra in a 1000–2600 nm region. This instrument was mainly used to measure the Tm^{3+} emission band at 1600–2100 nm. The excitation was undertaken by 785 nm laser diode. Absorption spectra of the crystal were measured with a Cary-5E spectrophotometer. The spectral resolution was set to be 0.2 nm. Emission and absorption spectra were measured at various temperatures between 12 K and 320 K.

3. Experimental results and discussion

3.1 IR emission bands

Figure 3 shows absorption spectra of TmYLF crystal at 12 and 287 K. The absorption bands consisting of sharp lines, which are due to the $4f^{12} \rightarrow 4f^{12}$ transition of Tm^{3+} , are observed in the 220–3100 nm spectral range. The bands at about 1600–1780, 1120–1230, 770–800, 680–700, 645–670, 450–480, 350–365, 285–290, 280–284, 270–275 and 255–264 nm in TmYLF are due to the electronic transitions from the ${}^3\text{H}_6$ ground state to the ${}^3\text{F}_4$, ${}^3\text{H}_5$, ${}^3\text{H}_4$, ${}^3\text{F}_3$, ${}^3\text{F}_2$, ${}^1\text{G}_4$, ${}^1\text{D}_2$, ${}^1\text{I}_6$, ${}^3\text{P}_0$, ${}^3\text{P}_1$ and ${}^3\text{P}_2$ states of Tm^{3+} , respectively^{9,12}. The YLF is transparent even at 200 nm, resulting in appearance of UV Tm^{3+} absorption bands associated with high energy levels such as the ${}^3\text{P}_2$ state. Various emission bands are observed at the IR to UV regions by the excitation into these states. Of them, the emission band at 1600–2000 nm is at the longest wavelength region in our measurement as shown in inset of Fig. 4. In the following we show various emission spectra in the IR to UV region.

Figure 4 shows the infrared emission spectra, at 12 K, of TmYLF excited by 780, 680, 460, 360 and 260 nm light. All of these excitations give rise to the same emission bands with peaks at 1510 and 1462 nm. On the other hand, two emission bands at 1229 and

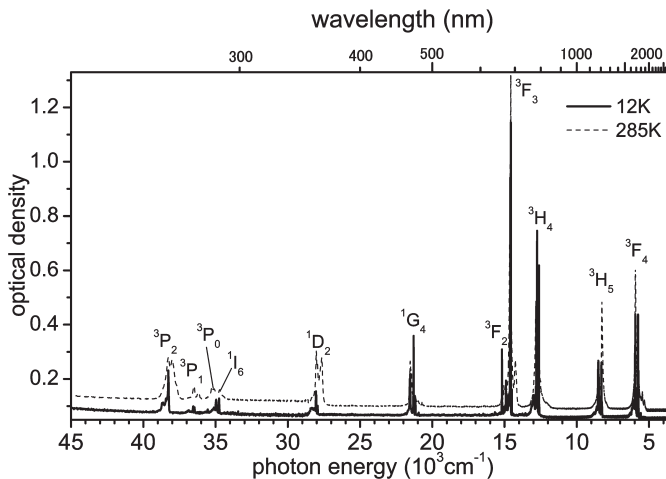


Fig. 3 Absorption spectra of a 6% Tm^{3+} -doped LiYF_4 crystal with a thickness of 2.70 mm at 12 and 285 K. The electronic term such as ${}^3\text{F}_4$, which is indicated on the absorption band, means the excited state responsible for the absorption band.

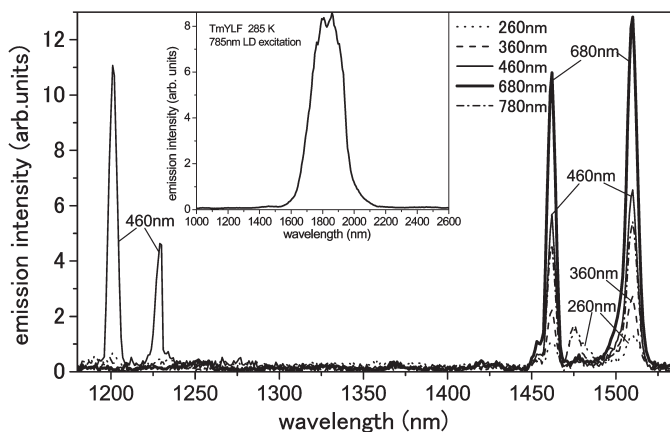


Fig. 4 Infrared emission spectra, at 12 K, of 6% Tm^{3+} -doped LiYF_4 crystal excited by 780, 680, 460, 360 and 260 nm lights. Inset shows another IR emission bands observed by 785 nm LD at 285 K using the ISM-140G spectrograph.

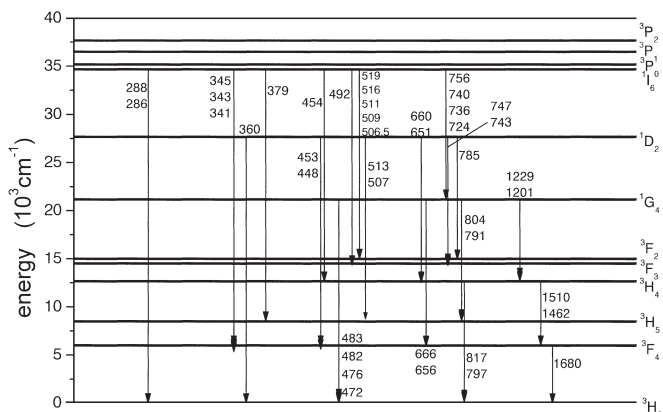


Fig. 5 Energy level diagram of Tm^{3+} and assignment of the observed Tm^{3+} emission bands in LiYF_4 crystal at 12 K.

1201 nm are observed under only the 460 nm excitation. They are also generated by the 360 and 260 nm excitations, but the intensities are much weaker than those generated by the 460 nm excitation. The 1229 and 1201 nm emission bands are not generated by the 780 and 680 nm excitations. The 1510 and 1462 nm emission bands are attributed to the ${}^3\text{H}_4 \rightarrow {}^3\text{F}_4$ transition from the energy level diagram of Tm^{3+} as shown in Fig. 5.

The 1229 and 1201 nm emission bands are observed by the 460, 360 and 260 nm excitations but not by the 780 and 680 nm excitations. Therefore these emission bands are attributed to the ${}^1\text{G}_4 \rightarrow {}^3\text{H}_4$ transition because the ${}^1\text{G}_4$ state is directly excited by the 460 nm light. The 360 and 260 nm light irradiation gives rise to the excitation into the ${}^1\text{D}_2$ and ${}^3\text{P}_2$ states directly, respectively, which locate at higher energy than the ${}^1\text{G}_4$ state. The 360 and 260 nm excitation does not give rise to intense emissions at 1229 and 1201 nm. After

the excitation into the $^1\text{D}_2$ and $^3\text{P}_2$ states, the Tm^{3+} ions are relaxed to the $^1\text{G}_4$ state from which the ions are relaxed to the lower states radiatively and non-radiatively. It is suggested that, unlike the case of direct excitation into the $^1\text{G}_4$ state, the branching ratio of the $^1\text{G}_4 \rightarrow ^3\text{H}_4$ radiative transition is much smaller than the other ratios.

3.2 Visible and UV emission bands

Figures 6 and 7 show the emission spectra at 780–830 and 650–760 nm at 12 K, respectively. Quite different emission spectra are observed depending on the excitation wavelength. Emission bands at 797, 817 and 822 nm are generated by the 260, 360, 460 and 680 nm excitations, emission band at 791 nm by the 260, 360 and 460 nm excitations, while emission band at 785 nm by only the 360 nm excitation, and emission band at 804 nm by only the 460 nm excitation. Therefore we can attribute the 797, 817 and 822 nm bands to the $^3\text{H}_4 \rightarrow ^3\text{H}_6$ transition, the 791 and 804 nm bands to the $^1\text{G}_4 \rightarrow ^3\text{H}_5$ transition, and the 785 nm band to the $^1\text{D}_2 \rightarrow ^3\text{F}_2$ transition (Fig. 5).

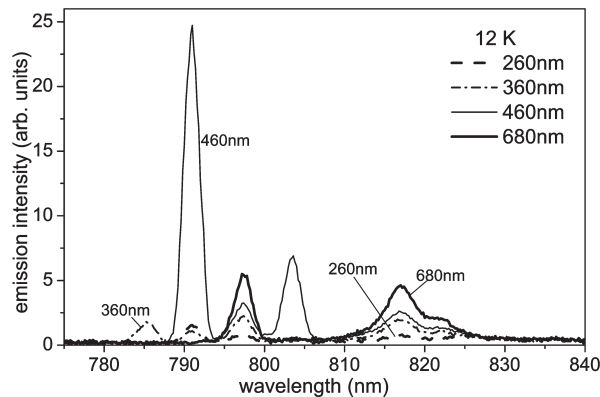


Fig. 6 Emission spectra of 6% Tm^{3+} -doped LiYF_4 crystal excited by 680, 460, 360 and 260 nm lights at 12 K.

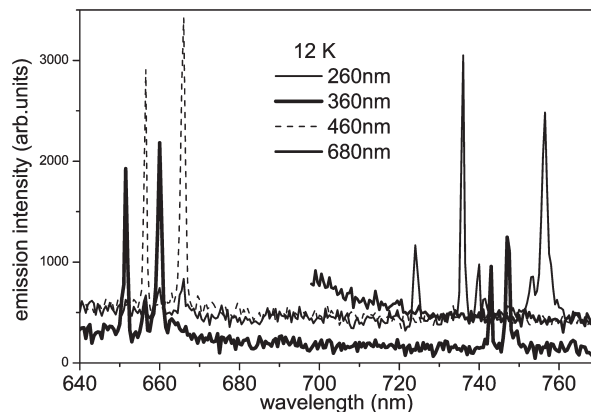


Fig. 7 Emission spectra of 6% Tm^{3+} -doped LiYF_4 crystal excited by 680, 460, 360 and 260 nm lights at 12 K.

As seen in Fig. 7 no emission band is observed in the 700–760 nm region by the 680 and 460 nm excitations. The 460 nm excitation gives rise to emission bands at 666 and 656.5 nm, the 360 nm excitation to emission bands at 747, 743, 660, 656.5 and 651 nm, while the 260 nm excitation to emission bands at 756.5, 740, 736, 724, 666, 660 and 656.5 nm. Therefore we can attribute the 756.5, 740, 736 and 724 nm bands to the transitions from the $^1I_6 \rightarrow ^1G_4$ transition, the 747 and 743 nm bands to the $^1D_2 \rightarrow ^3F_3$ transition, the 666 and 656 nm bands to the $^1G_4 \rightarrow ^3F_4$ transition, and the 660 and 651 nm bands to the $^1D_2 \rightarrow ^3H_4$ transition as shown in Fig. 5.

Figures 8 and 9 show the emission spectra at 470–525 and 292–460 nm at 12 K, respectively. The 460 nm excitation gives rise to emission bands at 490, 483.5, 481.5, 476 and 472 nm, the 360 nm excitation to emission bands at 513, 507, 453 and 448.5 nm, and the 260 nm excitation to emission bands at 519, 516, 511.5, 509.5, 506.5, 476, 454.5, 450.5, 379, 360, 349.5, 345.5, 343, 341, 288 and 286 nm. The assignment for these emission bands is possible from the energy level diagram of Tm^{3+} by the same method mentioned

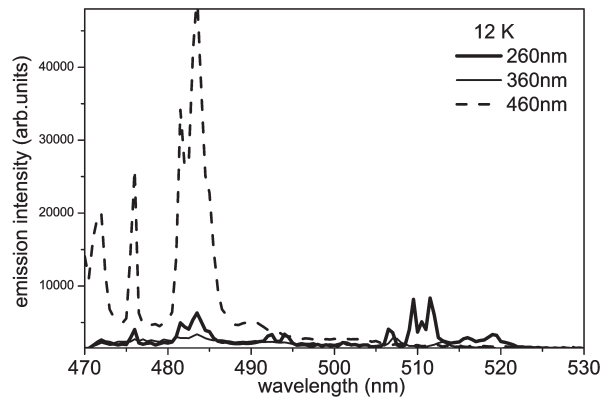


Fig. 8 Emission spectra of 6% Tm^{3+} -doped $LiYF_4$ crystal excited by 460, 360 and 260 nm lights at 12 K.

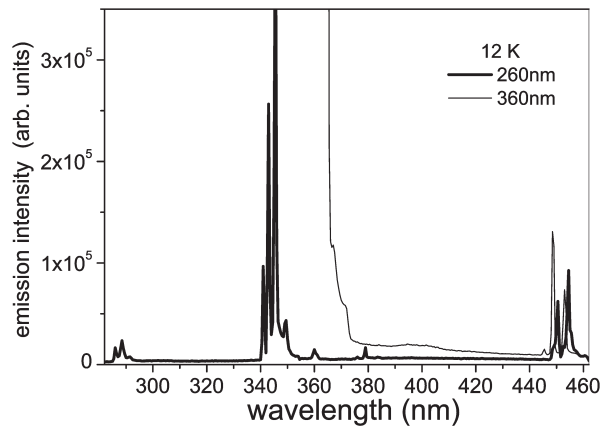


Fig. 9 Emission spectra of 6% Tm^{3+} -doped $LiYF_4$ crystal excited by 360 and 260 nm lights at 12 K.

above, which is shown in Fig. 5.

3.3 Excitation spectra for the IR and visible emission

Figure 10 shows the excitation spectrum in 250–850 nm region for the 1451 nm emission at 285 K. The excitation bands are the same as the absorption bands shown in Fig. 3. The same results were obtained for all the 1400–1520 nm emission bands shown in Fig. 1. This indicates that when the Tm^{3+} states above the $^3\text{H}_4$ state are excited all the states give rise to these IR emission bands. This is understood by the relaxation processes shown in Fig. 5.

Figure 11 shows the excitation spectra for the 791, 666 and 453 nm emissions at 12 K. Two intense bands at about 395 and 333 nm are due to the half harmonic of the 791 and 666 nm emission, respectively. The 791 nm emission is generated by the excitation of the

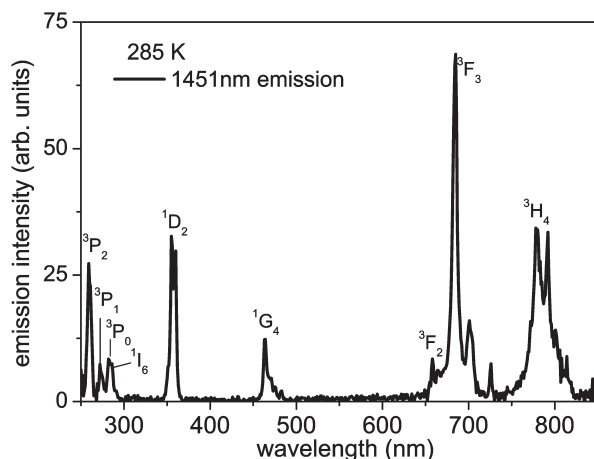


Fig. 10 Excitation spectrum for 1451 nm emission of 6% Tm^{3+} -doped LiYF_4 crystal at 285 K.

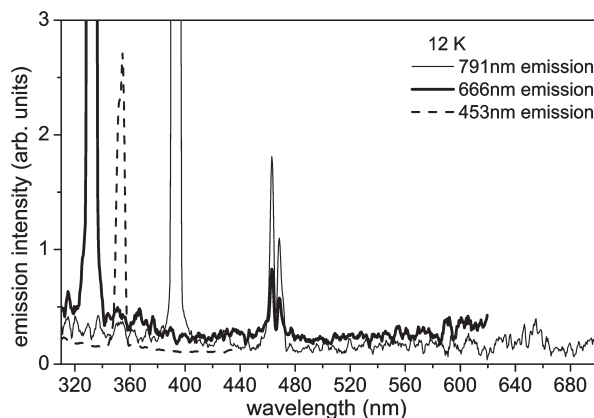


Fig. 11 Excitation spectrum for 791, 666 and 453 nm emissions of 6% Tm^{3+} -doped LiYF_4 crystal at 12 K.

460–470 nm absorption bands (due to the ${}^3\text{H}_6 \rightarrow {}^1\text{G}_4$ transition), but it is not generated by the excitation of the 355–360 nm absorption bands (due to the ${}^3\text{H}_6 \rightarrow {}^1\text{D}_2$ transition). Unlike the 797 and 817 nm emission bands, the 791 nm emission is not generated by the excitation of the 660–700 nm absorption bands (due to the ${}^3\text{H}_6 \rightarrow {}^3\text{F}_2$ and ${}^3\text{F}_3$ transitions). This indicates that neither the multi-phonon non-radiative process nor radiative transition occurs in the relaxation from the ${}^1\text{D}_2$ excited state into the nearby lower-energy state ${}^1\text{G}_4$.

Regarding the 666 nm emission, it is generated by the excitation of the 460–470 nm absorption bands (due to the ${}^3\text{H}_6 \rightarrow {}^1\text{G}_4$ transition). Unlike the 660 and 651 nm emission bands, it is not generated by the excitation of the 355–360 nm absorption bands (due to the ${}^3\text{H}_6 \rightarrow {}^1\text{D}_2$ transition). This shows that the different electronic transition is responsible between the 666 and 660 nm emission bands although these emission wavelengths are close to each other. Therefore our level assignment for the 666 and 660 nm emission bands (shown in Fig. 5) is confirmed by the excitation spectra and the absence of both non-radiative and radiative transitions from the ${}^1\text{D}_2$ state to the ${}^1\text{G}_4$ state, because, if one of such transitions occur, the 666 nm emission should be generated by the excitation into the ${}^1\text{D}_2$ state with 355–360 nm light.

Regarding the 453 nm emission, it is generated by the excitation into the 355–360 nm band (due to the ${}^3\text{H}_6 \rightarrow {}^1\text{D}_2$ transition). We assigned this emission to the ${}^1\text{D}_2 \rightarrow {}^3\text{F}_4$ transition from the emission spectrum measurement (Fig. 5). This is consistent with the result of excitation spectrum. In this way we can confirm of the optical process shown in Fig. 5 by the excitation spectra.

4. Summary

Photoluminescence and excitation spectra of Tm^{3+} ions in LiYF_4 crystal have been investigated at 12 K. The photoluminescence appeared in infrared, visible and ultraviolet regions is investigated under excitation with lights of 780, 680, 460, 360 and 266 nm wavelengths. Two emission bands are observed at 1510 and 1462 nm in the 1400–1550 nm region. No difference is observed for these bands among the 780, 680, 460, 360 and 266 nm excitations, while two emission bands at 1229 and 1201 nm are generated by the 460 nm excitation but not by 780 and 680 nm excitations. Such a dependence of emission bands on the excitation wavelength is observed in various emission bands from near-IR to UV region. Comparing with the results of excitation spectra, we suggest the level assignment for all the observed luminescence bands. For example, the 666 and 656 nm bands are attributed to the ${}^1\text{G}_4 \rightarrow {}^3\text{F}_4$ transition, while the 660 and 651 nm bands, which locate close to the 666 and 656 nm bands, to the ${}^1\text{D}_2 \rightarrow {}^3\text{H}_4$ transition.

References

- 1) G. L. Bourdet, G. Lescroart and R. Muller, *Opt. Commun.* **150** (1998) 141.
- 2) F. Cornacchia, A. Di Lieto, P. Maroni, P. Minguzzi, A. Toncelli, M. Tonelli, E. Sorokin, and I. T. Sorokina, *Appl. Phys. B* **73** (2001) 191.

- 3) V. Sudesh, K. Asai, K. Shimamura and T. Fukuda, *IEEE J. Quant. Electr.* **38** (2002) 1102.
- 4) V. Sudesh and K. Asai, *J. Opt. Soc. Am. B* **20** (2003) 1829.
- 5) T. Komukai, T. Yamamoto, T. Sugawa and Y. Miyajima, *IEEE J. Quant. Electr.* **31** (1995) 1880.
- 6) S. Kawanishi, K. Uchiyama, H. Takara, T. Morioka, M. Yamada and T. Kanamori, *Electron. Lett.* **33** (1997) 1553.
- 7) G. Özen and B. Di Bartolo, *Appl. Phys. B*, **70** (2000) 189.
- 8) G. Özen and S. Salihoglu, *Optics Commun.* **180** (2000) 323.
- 9) A. Brener, J. Rubin, R. Moncorge and C. Pedrini, *J. Physique*, **50** (1989) 1463.
- 10) T. Tsuboi, Y.F. Ruan and N. Kulagin, *Physics of Laser Crystals*, NATO SCIENCE SERIES: II: Mathematics, Physics and Chemistry Vol. 126, edited by J. C. Krupa and N. A. Kulagin (Kluwer Sci. Publ., London), Chapt. **12**, 171–185, 2003.
- 11) T. Tsuboi, M. Tanigawa and K. Shimamura, *Opt. Commun.* **186** (2000) 127.
- 12) T. Tsuboi, *J. Electrochem. Soc.* **147** (2000) 1997.
- 13) J. Sytsma, G. F. Imbusch, G. Blasse, *J. Phys.: Cond. Matt.* **2** (1990) 5171.